AD A0 60 688

DDC FILE COPY

SECURITY CLASSIFICATION OF THIS PAGE (When Data Entered)

REPORT DOCUMENTATION PAGE		READ INSTRUCTIONS BEFORE COMPLETING FORM
1. REPORT NUMBER	2. GOVT ACCESSION NO.	3. RECIPIENT'S CATALOG NUMBER
4. TITLE (and Subtitle) (6) Theory of Damped Surface Magnetoplasmons in n-Type InSb		5. TYPE OF REPORT & PERIOD COVERED (9) FINAL rept.
		6. PERFORMING ORG. REPORT NUMBER (14) TR-78-9
7. AUTHOR(s) (10) B. G. Martin, A. A. Maradudin [redacted] R. F. Wallis	(12)	8. CONTRACT OR GRANT NUMBER(s) (15) N00014-76-C-0121
9. PERFORMING ORGANIZATION NAME AND ADDRESS University of California, Irvine Irvine, CA 92717		10. PROGRAM ELEMENT, PROJECT, TASK AREA & WORK UNIT NUMBERS NR 392-001
11. CONTROLLING OFFICE NAME AND ADDRESS Office of Naval Research Physics Program 800 N. Quincy St. Arlington, VA 22217		12. REPORT DATE (11) 1976
		13. NUMBER OF PAGES 24 (12) 25p.
14. MONITORING AGENCY NAME & ADDRESS (if different from Controlling Office) LEVEL II		15. SECURITY CLASS. (of this report) UNCLASSIFIED
		15a. DECLASSIFICATION/DOWNGRADING SCHEDULE

16. DISTRIBUTION STATEMENT (of this Report)

Approved for public release; distribution unlimited

17. DISTRIBUTION STATEMENT (of the abstract entered in Block 20, if different from Report)

DDC
RECEIVED
NOV 2 1978
F

18. SUPPLEMENTARY NOTES

19. KEY WORDS (Continue on reverse side if necessary and identify by block number)

Surfaces, Magnetoplasma waves, Surface Polaritons, Indium Antimonide

20. ABSTRACT (Continue on reverse side if necessary and identify by block number)

A theoretical investigation of surface magnetoplasmons in n-type InSb has been carried out with the effect of damping taken into account. Part of the investigation included surface magnetoplasmons interacting with surface optical phonons. The calculated dispersion curves show backbending, in contrast to the situation where damping is neglected. In addition, there are gaps in the dispersion curves for certain frequency ranges.

DD FORM 1 JAN 73 1473

UNCLASSIFIED

SECURITY CLASSIFICATION OF THIS PAGE (When Data Entered)

387 300 78 10 23 142 JOB

THEORY OF DAMPED SURFACE MAGNETOPLASMONS IN n-TYPE InSb*

B. G. Martin, A. A. Maradudin, and R. F. Wallis

University of California, Irvine

Abstract

A theoretical investigation of surface magnetoplasmons in n-type InSb has been carried out with the effect of damping taken into account. Part of the investigation included surface magnetoplasmons interacting with surface optical phonons. The calculated dispersion curves show backbending, in contrast to the situation where damping is neglected. In addition, there are gaps in the dispersion curves for certain frequency ranges.

* Work supported in part by the Office of Naval Research under Grant No. N00014-76-C-0121

Technical Report #78-9

INTRODUCTION

Brion et al.[1] have made a theoretical investigation of surface magnetoplasmons in n-type InSb with the magnetic field parallel to the surface and the wave vector perpendicular to the magnetic field direction. They obtained the interesting result that a gap may appear in the surface magnetoplasmon dispersion curve; however, they neglected the effect of damping. Brion et al.[2] have also made a theoretical investigation of the effects of a magnetic field on interacting surface plasmons and surface optical phonons, again neglecting damping.

Experimentally, damping is always present due to the scattering of the free carriers by defects or phonons. In the present investigation, we have therefore obtained the surface magnetoplasmon dispersion relation in the presence of free carrier damping. The interaction with surface optical phonons is also considered. Dispersion curves are presented for n-type InSb, using the same values of the pertinent parameters as were used by Brion et al.[1,2]. The results are compared with those of Brion et al.

THEORY

We will first obtain the dielectric tensor including damping. In what follows, the static magnetic field $\vec{B}_o$ is taken to be parallel to the surface (which lies in the xy-plane) and pointing in the y-direction. In addition, we take the magnetoplasmon wave vector to be perpendicular to $\vec{B}_o$. The geometrical arrangement is shown in Fig. 1.

We begin with the equation of motion

$$m^* \frac{d\vec{v}}{dt} + m^* \nu \vec{v} = -e\vec{E} - \frac{e}{c}(\vec{v} \times \vec{B}_o) \qquad (1)$$

where m^* is the electron effective mass, $\vec{v}$ is the velocity, ν is the damping constant, $\vec{E}$ is the electric field, and $-e$ is the electronic charge. It is assumed that

$$\vec{v} = \vec{v}_o \, e^{-i\omega t} \tag{2}$$

and

$$\vec{E} = \vec{E}_o \, e^{-i\omega t} \quad . \tag{3}$$

Substituting these values into Eq. (1), we solve for $\vec{v}$ in terms of $\vec{E}$. The conductivity tensor $\overleftrightarrow{\sigma}$ can then be obtained from the defining equation

$$\vec{J} \equiv - N_o e \vec{v} = \overleftrightarrow{\sigma} \cdot \vec{E} \tag{4}$$

where N_o is the free carrier density and $\vec{J}$ is the current density.

The dielectric tensor follows from the equation

$$\overleftrightarrow{\epsilon} = \epsilon^p \, \overleftrightarrow{I} + \frac{4\pi i}{\omega} \, \overleftrightarrow{\sigma} \, , \tag{5}$$

where ϵ^p contains contributions to the dielectric tensor other than from free carriers and $\overleftrightarrow{I}$ is the 3 x 3 unit tensor. In component form, we have

$$\overleftrightarrow{\epsilon} = \begin{pmatrix} \epsilon_{xx} & 0 & \epsilon_{xz} \\ 0 & \epsilon_{yy} & 0 \\ \epsilon_{zx} & 0 & \epsilon_{zz} \end{pmatrix} \quad , \tag{6}$$

where

$$\epsilon_{xx}(\omega) = \epsilon^p - \frac{\epsilon_\infty \omega_p^2}{\omega} \cdot \frac{\omega + i\nu}{(\omega+i\nu)^2 - \omega_c^2} = \epsilon_{zz}(\omega), \tag{7a}$$

$$\epsilon_{xz}(\omega) = \frac{i\epsilon_\infty \omega_p^2}{\omega} \cdot \frac{\omega_c}{(\omega+i\nu)^2 - \omega_c^2} = -\epsilon_{zx}(\omega) , \tag{7b}$$

$$\epsilon_{yy}(\omega) = \epsilon^p - \frac{\epsilon_\infty \omega_p^2}{\omega} \cdot \frac{1}{\omega+i\nu} . \tag{7c}$$

In these expressions, ω_c is the cyclotron frequency given by eB_o/m^*c, ω_p is the plasma frequency given by $4\pi N_o e^2/m^*\epsilon_\infty$, and ϵ_∞ is the background dielectric constant.

Two values for the quantity ϵ^p are considered. The situation where the interaction between surface optical phonons and magnetoplasmons occurs can be handled in a simple manner by setting

$$\epsilon^p = \epsilon_\infty \left(1 + \frac{\omega_L^2 - \omega_T^2}{\omega_T^2 - \omega^2} \right) , \tag{8}$$

where ω_L and ω_T are the long wavelength longitudinal and transverse optical phonon frequencies, respectively. Damping of the optical phonons is neglected because this is small compared to the electronic damping for the case considered. In addition, the limiting case

$$\epsilon^{p} = \epsilon_{\infty} \tag{9}$$

is also considered. This corresponds to the situation where the effect of optical phonons is neglected.

Consider next the electric and magnetic fields of the radiation. The electric field components will be expressed as

$$E_{\alpha}(\vec{x},t) = E_{\alpha}(z)e^{ik_x x - i\omega t} \quad , \tag{10}$$

with similar forms for the displacement field $\vec{D}$ and magnetic field $\vec{H}$. Substituting these forms into the $\vec{\nabla} \times \vec{E}$ and $\vec{\nabla} \times \vec{H}$ Maxwell equations and eliminating $\vec{H}$, one obtains equations relating the x-, y-, and z-components of $\vec{E}$ and $\vec{D}$. To complete the set of equations, one needs the relations between $\vec{D}$ and $\vec{E}$ in the crystal ($z > 0$) and in the vacuum ($z < 0$); these are

$$D_{\alpha}(z) = \sum_{\beta} \epsilon_{\alpha\beta}(\omega)E_{\beta}(z) \tag{11}$$

and

$$D_{\alpha}(z) = E_{\alpha}(z) \quad , \tag{12}$$

respectively.

For surface magnetoplasmons for the geometry stated, we need consider only p-polarization, i.e., the electric vector lies in the sagittal plane. For this situation, $E_y(z) = 0$, and we obtain the following coupled differential equations:

$$-\frac{d^2}{dz^2}E_x(z) + ik_x\frac{d}{dz}E_z(z) = \frac{\omega^2}{c^2}\epsilon_{xx}(\omega)E_x(z) + \frac{\omega^2}{c^2}\epsilon_{xz}(\omega)E_z(z) \qquad (13)$$

$$ik_x\frac{d}{dz}E_x(z) + k_x^2 E_z(z) = \frac{\omega^2}{c^2}\epsilon_{zx}(\omega)E_x(z) + \frac{\omega^2}{c^2}\epsilon_{zz}(\omega)E_z(z) \qquad (14)$$

If it is assumed that

$$E_x(z) = A_1 e^{-\alpha z},\ E_z(z) = A_2 e^{-\alpha z},\ z \geq 0, \qquad (15)$$

one obtains from Eqs. (13) and (14) the following expression for the decay constant α:

$$\alpha^2 = k_x^2 - \frac{\omega^2}{c^2}\left(\epsilon_{xx} + \frac{\epsilon_{xz}^2}{\epsilon_{xx}}\right) . \qquad (16)$$

The constants A_1 and A_2 are related by the equation

$$A_2 = A_1\left(\frac{ik_x\alpha - \frac{\omega^2}{c^2}\epsilon_{xz}}{k_x^2 - \frac{\omega^2}{c^2}\epsilon_{xx}}\right) . \qquad (17)$$

Consider next the fields in the vacuum. Proceeding as before and assuming that

$$E_x(z) = A_3 e^{\alpha_o z},\ E_z(z) = D_z(z) = A_4 e^{\alpha_o z},\ z < 0, \qquad (18)$$

one obtains the results

$$\alpha_o^2 = k_x^2 - \frac{\omega^2}{c^2} \qquad (19)$$

and

$$A_4 = \frac{-ik_x}{\alpha_o} A_3 . \qquad (20)$$

By applying the boundary conditions of continuity of $E_x(z)$ and $D_z(z)$ at $z = 0$, we obtain the surface magnetoplasmon dispersion relation

$$\frac{1}{\alpha_o} + \frac{ik_x\epsilon_{xz} + \alpha\epsilon_{xx}}{k_x^2 - \frac{\omega^2}{c^2}\epsilon_{xx}} = 0 \quad . \qquad (21)$$

RESULTS AND DISCUSSION

Theoretical dispersion curves have been obtained for surface magnetoplasmons where the effects of both damping and retardation have been included. The situation whe[illegible]ace optical phonons interact with damped surface magnetoplasm[illegible]s also been investigated.

Calculations were made using values of parameters appropriate for n-type InSb. For the case of surface magnetoplasmons alone, which will be considered first, we take $\epsilon^p = \epsilon_\infty$, i.e., we neglect the contribution of surface optical phonons. The value used for the background dielectric constant ϵ_∞ was 15.68[3] and the value of the ratio $|\omega_c/\omega_p|$ was taken to be 0.5. Two values of the damping parameter were considered: $\nu = 0.01\ \omega_p$ and $0.1\omega_p$. For comparison, the results of Brion et al.[1,2] for $\nu = 0$ are also presented.

In making the calculations, real values of ω/ω_p were assumed and complex values of the wave vector $k_x (= k_1 + ik_2)$ and the decay constant $\alpha (= \alpha_1 + i\alpha_2)$ were calculated using a digital computer.

The values of ω/ω_p were taken in steps of 0.01 or smaller for the range $0 \leq \omega/\omega_p \leq 1.75$. The computer program calculated the complex values of k_x using Muller's method[4], a process of successive approximations from initial guesses (which need not be externally supplied).

Figure 2 shows the surface magnetoplasmon dispersion curves for $\nu/\omega_p = 0.01$ for both $\omega_c > 0$ and $\omega_c < 0$. Figure 3 shows the corresponding frequency dependence of the imaginary part of the wave vector associated with surface magnetoplasmons. Figures 4 and 5 give the same type of results for $\nu/\omega_p = 0.1$. Figures 2 and 4 also show the dispersion curves for $\nu = 0$ (dash-dash curves).

The interaction of surface magnetoplasmons and surface optical phonons is considered next. This interaction occurs for electron concentrations of $\gtrsim 10^{17}\ cm^{-3}$. The plasma frequency ω_p was chosen so that the transverse optical phonon frequency ω_T lies in the gap of the surface magnetoplasmon dispersion curve for $\nu = 0$ (see Fig. 2). Figures 6 and 7 show the dispersion curves for $\omega_c > 0$ and $\omega_c < 0$, respectively, for $\nu/\omega_p = 0.1$. As in the preceding figures, the curves for $\nu = 0$ are also shown. Figure 8 shows the frequency dependence of the imaginary part of the wave vector associated with surface magnetoplasmons interacting with surface optical phonons.

In Fig. 2, for $\nu = 0$, we see that for the two signs of ω_c (or, equivalently, the two signs of k_x), the dispersion curves differ for most of the frequency range considered. Consider first the case for $\omega_c > 0$. The dispersion curve consists of two branches with a gap between them, i.e., the single branch that would occur for zero magnetic field (not shown) is split into two branches when a sufficiently large magnetic field is applied. The lower branch[1] of the surface magnetoplasmon dispersion curve terminates when it intersects the dispersion curve for bulk magnetoplasmons defined by $\alpha' = 0$ where α' is the value of α when $\nu = 0$. The upper branch[1] begins on the line defined by $\epsilon_{xx} = 0$, and approaches asymptotically the frequency defined by the equation $1 + \epsilon_{xx} - i\epsilon_{xz} = 0$, this being the frequency for unretarded surface magnetoplasmons found by Pakhomov and Stepanov[5]. Brion et al.[1] have shown that for the gap to occur, the dielectric constant ϵ_∞ must satisfy the inequality $\epsilon_\infty > (\omega_c^2 + \omega_p^2)^{\frac{1}{2}}/\omega_c$.

Consider next the case for $\omega_c < 0$. Again for non-zero magnetic field there are two branches in the surface magnetoplasmon dispersion curve with a gap separating them. The lower branch[1] approaches the asymptotic frequency value given by the equation $1 + \epsilon_{xx} + i\epsilon_{xz} = 0$. The upper branch[1] starts at the light line at the point where $\epsilon_{xx} = 1$, and terminates when it intersects the upper bulk magnetoplasmon dispersion curve $\alpha' = 0$. Figure 2 shows that the addition of damping ($\nu = 0.01\omega_p$) causes changes, relative to the $\nu = 0$ situation, for both signs of ω_c. For $\omega_c > 0$, there are three branches. The lower branch coincides with the corresponding $\nu = 0$ branch until the former terminates at $\alpha_1 = 0$, just before intersecting the line $\alpha' = 0$ (α_1 is nearly equal to α' since the damping ν is small). Then there is a gap followed by the second branch which begins at $\alpha_1 = 0$, just to the left of the light line, and continues upward until it intersects the light line, at which point it terminates. There is then another gap followed by the third branch which begins at the light line near $\epsilon_{xx} = 1$ and essentially follows the corresponding $\nu = 0$ curve as it approaches the line $1 + \epsilon_{xx} - i\epsilon_{xz} = 0$.

For $\omega_c < 0$, there are two branches. The lower branch is essentially coincident with the $\nu = 0$ curve until it almost reaches the asymptotic line $1 + \epsilon_{xx} = i\epsilon_{xz} = 0$. Then it quickly bends back, crosses the light line, and terminates at a point where $k_2 = 0$, i.e., where the imaginary part of the surface polariton wave vector vanishes. A large gap occurs, and then the second branch begins at the light line at $k_2 = 0$, near $\epsilon_{xx} = 1$. It initially follows the $\nu = 0$ curve, then backbends across the light line, doubles back slightly, and subsequently proceeds nearly parallel to the light line. The backbending is analogous to the situation that occurs for Ge[(6)].

Figure 3 shows the frequency dependence of the imaginary part of the wave vector for both signs of ω_c. Note by comparing Figs. 2 and 3 that when the k_1 curves reverse direction, the k_2 curves also reverse direction. In a sense, the k_2 curves track the k_1 curves. This type of behavior has also been noted before[(6)].

Figure 4 shows the effect on the surface magnetoplasmons of increasing the damping by one order of magnitude, i.e., increasing the damping to $\nu = 0.1\omega_p$. Note that, as compared to the result for $\nu = 0.01\omega_p$ in Fig. 2, the curve for $\nu = 0.1\omega_p$ ($\omega_c > 0$) in Fig. 4 fills in the gaps between the first and second and between the second and third branches, and then terminates to the left of the light line at $k_2 = 0$. The lower branch of the $\omega_c < 0$ curve moves to the right of the light line to a much lesser extent for $\nu/\omega_p = 0.1$ (Fig. 4) than for $\nu = 0.01\ \omega_p$ (Fig. 2) before backbending and terminating at $k_2 = 0$. The upper branch of the $\omega_c < 0$ curve for $\nu = 0.1\ \omega_p$ begins at the light line at $k_2 = 0$ near $\epsilon_{xx} = 0$, moves upward near the light line, and then backbends slightly. Subsequently, it moves essentially parallel to the light line in the same manner as for $\nu = 0.01\ \omega_p$ (Fig. 2).

The frequency dependence of the imaginary part of the wave vector shown in Fig. 5 for $\nu = 0.1\ \omega_p$ essentially tracks the behavior of the frequency dependence of the real part of the wave vector shown in Fig. 4.

Next, consider the interaction of surface magnetoplasmons and surface optical phonons in n-type InSb. Brion et al.[2] found that this interaction, for the case of $\nu = 0$, leads to interesting results if the unretarded surface optical phonon frequency ω_s, given by

$$\omega_s = \left\{ \omega_T^2 + \frac{\omega_L^2 - \omega_T^2}{1 + 1/\epsilon_\infty} \right\}^{\frac{1}{2}} , \qquad (22)$$

is located in the gap region for surface magnetoplasmons alone.

Figure 6 shows the dispersion curves ($\omega_c > 0$) that result when the magnetoplasmon-optical phonon interaction is included. For $\nu = 0$, the interaction has the effect of doubling the number of branches (compare Fig. 6 with Fig. 4). In Fig. 6, the lower branch starts at zero and moves to the right of the light line until it intersects a bulk dispersion curve (one of the roots of $\alpha' = 0$). The second branch starts at the light line at one of the roots of $\epsilon_{xx} = 0$ and then flattens out asymptotically as indicated in the figure. The third branch starts at the light line at ω_T(excluding, however, the point $\omega = \omega_T$) and terminates when it intersects a bulk dispersion curve($\alpha' = 0$). Finally, the fourth branch begins at the light line at $\epsilon_{xx} = 0$ and then flattens out asymptotically as indicated.

The inclusion of damping ($\nu = 0.1\omega_p$), as is now to be expected, causes the dispersion curves to backbend across the light line. In addition, there are now only two branches instead of four. The lower branch at first coincides with the $\nu = 0$ branch, backbends in the vicinity of $\alpha' = 0$, crosses the light line, has a dimple which carries it just to the right of the light line at a frequency just below ω_T, and then terminates at $\omega = \omega_T$ (also at this point, $k_2 = 0$). The next branch starts at the light line at $\omega = \omega_T$ and initially follows the $\nu = 0$ curve. Near $\alpha' = 0$, however, this branch backbends, crosses the light line to the left, recrosses the light line to the right, and finally backbends to the left of the light line terminating at $k_2 = 0$.

Figure 7 shows the surface magnetoplasmon-surface optical phonon dispersion curves for $\omega_c < 0$. As for the case just discussed ($\omega_c > 0$), the surface magnetoplasmon-surface optical phonon interaction results in doubling the number of branches for $\nu = 0$ (compare Fig. 7 with Fig. 4). In addition, the branches behave in a manner very similar to that where $\omega_c > 0$.

The addition of damping for $\omega_c < 0$ (Fig. 6) leaves the number of branches at four. The first branch initially tracks the $\nu = 0$ case; it then backbends and terminates at $k_2 = 0$.

The second branch is short, starting just to the left of the light line where $k_2 = 0$, showing a dimple which carries it just to the right of the light line at a frequency just below ω_T, and terminating at $\omega = \omega_T$, where also $k_2 = 0$. The third branch starts at $\omega = \omega_T$, moves slightly to the right of the light line, backbends and then terminates at $k_2 = 0$. Finally, the fourth branch begins at the light line at $k_2 = 0$, and moves essentially along the light line, but slightly to the right. It subsequently backbends to the left of, and then moves parallel to, the light line.

Figure 8 shows the corresponding frequency dependence of the imaginary part of the wave vector. The behavior is similar to that noted previously.

Although we have not carried out an exhaustive investigation of the effects of damping on surface magnetoplasmon dispersion curves, our results demonstrate that damping produces backbending of the type found in previous investigations[6,7] when the frequency is taken to be real and the wave vector is taken to be complex. As a consequence of the backbending, portions of the dispersion curves lie to the left of the light line $\omega = ck$, and the corresponding modes are known as Zenneck modes.[8]

Another effect produced by damping is a tendency to reduce or eliminate gaps in the dispersion curves as the damping is increased. This is clearly illustrated in Fig. 4 for $\nu = 0.1\omega_p$ where the gap in the dispersion curve for $\omega_c > 0$ has been completely eliminated.

Some comment on the relationship of our results to the experimental work of Hartstein and Burstein[9] is in order. In their determination of the surface magnetoplasmon dispersion curves for n-type InSb using attenuated total reflection, they observed no backbending. This result may be understood in terms of the discussion of Kovener et al.[7] who point out that dispersion curves determined by varying the incident angle at fixed ω should show backbending, while those determined by varying ω at fixed incident angle should not show backbending. Since Hartstein and Burstein carried out their experiments by varying ω at fixed incident angle, their procedure falls into the second category just mentioned, and it is reasonable that they did not observe backbending. It would be interesting, however, to carry out experiments to reveal the backbending by varying the incident angle at fixed ω.

REFERENCES

1. J. J. Brion, R. F. Wallis, A. Hartstein, and E. Burstein, Phys. Rev. Lett. 28 (1972) 1455.

2. J. J. Brion, R. F. Wallis, A. Hartstein, and E. Burstein, Surf. Sci. 34 (1973) 73.

3. M. Hass and B. W. Henvis, J. Phys. Chem. Solids 23 (1962) 1099.

4. D. E. Muller, Math. Tab. Wash. 10 (1956) 208.

5. V. I. Pakhomov and K. N. Stepanov, Zh. Tekh. Fiz. 37 (1967) 1393 [Sov. Phys. Tech. Phys. 12 (1968) 1011].

6. B. G. Martin and R. F. Wallis, Phys. Rev. B 13 (1976) 3339.

7. G. S. Kovener, R. W. Alexander, and R. J. Bell, Phys. Rev. B14 (1976) 3339.

8. J. Zenneck, Ann, Phys. 23 (1907) 846.

9. A. Hartstein and E. Burstein, Solid State Commun. 14 (1974) 1223.

FIGURE CAPTIONS

1. The coordinate system and specimen geometry.
2. Dispersion curves for surface magnetoplasmons in n-type InSb ($\nu/\omega_p = 0.01$). The dash - dash curves are the dispersion curves for $\nu/\omega_p = 0.0$.
3. The frequency dependence of the imaginary part of the wave vector associated with surface magnetoplasmons in n-type InSb ($\nu/\omega_p = 0.01$).
4. Dispersion curves for surface magnetoplasmons in n-type InSb ($\nu/\omega_p = 0.1$). The dash - dash curves are the dispersion curves for $\nu/\omega_p = 0.0$.
5. The frequency dependence of the imaginary part of the wave vector associated with surface magnetoplasmons in n-type InSb ($\nu/\omega_p = 0.1$).
6. Dispersion curves for surface magnetoplasmons in n-type InSb where the interaction with surface optical phonons is included ($\omega_c>0$). The dash - dash curves are the dispersion curves for $\nu/\omega_p = 0.0$.
7. Dispersion curves for surface magnetoplasmons in n-type InSb, where the interaction with surface optical phonons is is included ($\omega_c<0$). The dash - dash curves are the dispersion curves for $\nu/\omega_p = 0.0$.
8. The frequency dependence of the imaginary part of the wave vector associated with surface magnetoplasmons in n-type InSb where the interaction with surface optical phonons is included.

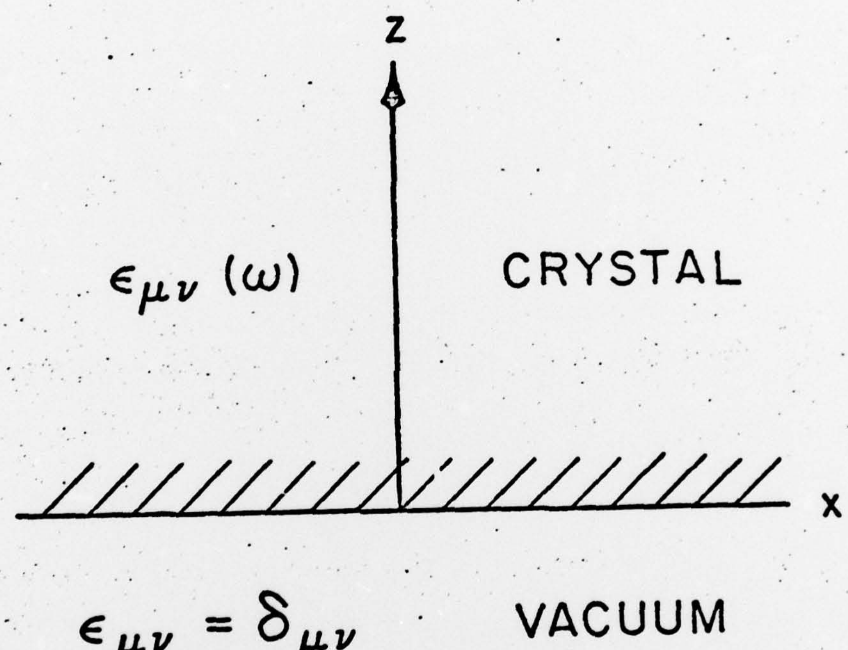
z
$\epsilon_{\mu\nu}(\omega)$
CRYSTAL
x
$\epsilon_{\mu\nu} = \delta_{\mu\nu}$
VACUUM

Fig. 1

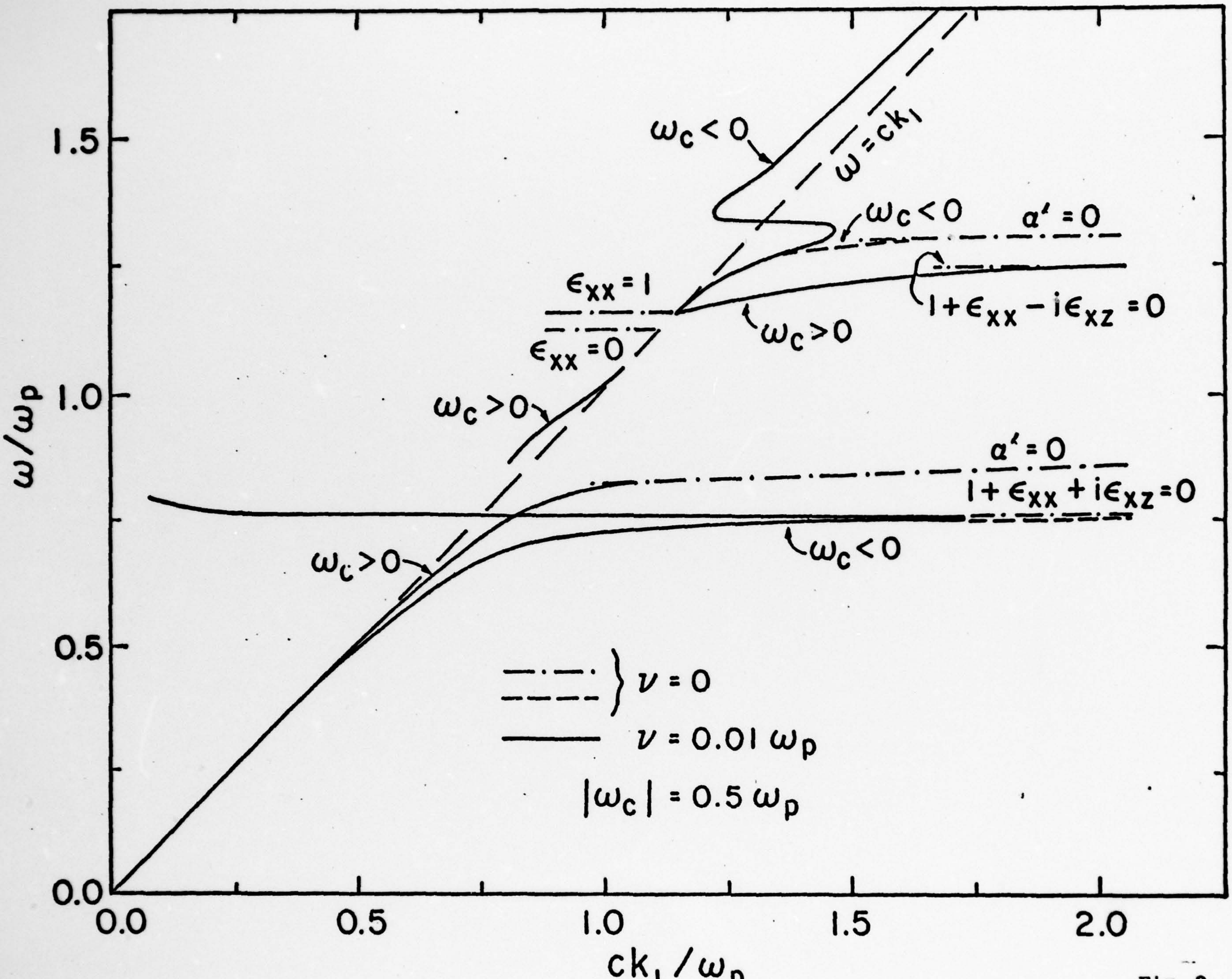
ω/ω_p
ck_1/ω_p
0.0
0.5
1.0
1.5
2.0
ω = ck_1
ω_c < 0
ω_c < 0
ω_c > 0
ω_c > 0
ω_c > 0
ω_c < 0
α' = 0
α' = 0
ε_xx = 1
ε_xx = 0
1 + ε_xx − iε_xz = 0
1 + ε_xx + iε_xz = 0
ν = 0
ν = 0.01 ω_p
|ω_c| = 0.5 ω_p

Fig. 2

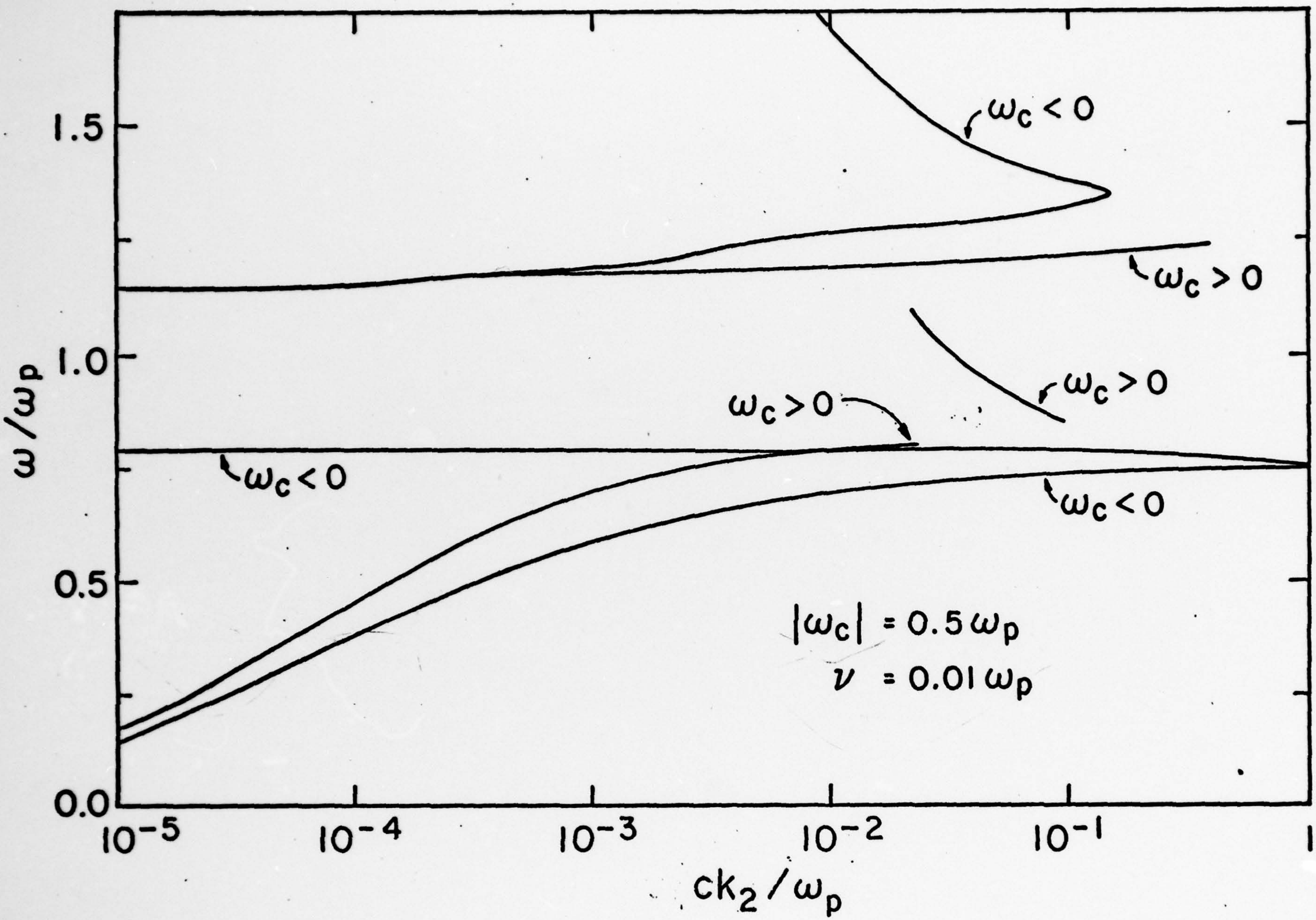

$\omega_c < 0$
$\omega_c > 0$
$\omega_c > 0$
$\omega_c > 0$
$\omega_c < 0$
$\omega_c < 0$
$|\omega_c| = 0.5\,\omega_p$
$\nu = 0.01\,\omega_p$
1.5
1.0
0.5
0.0
ω / ω_p
10^{-5}
10^{-4}
10^{-3}
10^{-2}
10^{-1}
1
ck_2 / ω_p

Fig. 3

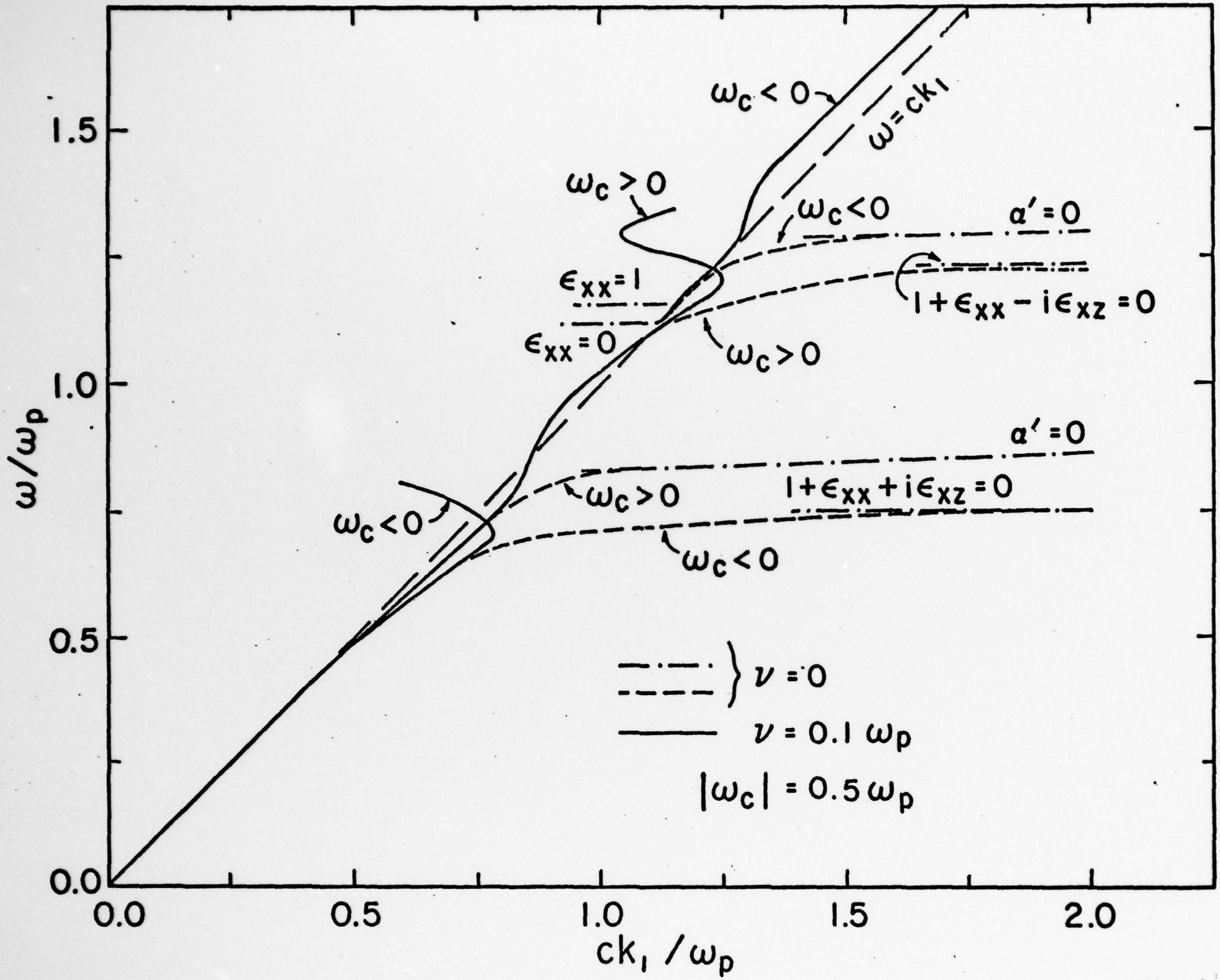

$\omega_c < 0$
$\omega = ck_1$
$\omega_c > 0$
$\omega_c < 0$
$\alpha' = 0$
$\epsilon_{xx} = 1$
$1 + \epsilon_{xx} - i\epsilon_{xz} = 0$
$\epsilon_{xx} = 0$
$\omega_c > 0$
$\alpha' = 0$
$\omega_c > 0$
$1 + \epsilon_{xx} + i\epsilon_{xz} = 0$
$\omega_c < 0$
$\omega_c < 0$
$\nu = 0$
$\nu = 0.1\ \omega_p$
$|\omega_c| = 0.5\ \omega_p$
ω/ω_p
ck_1/ω_p
0.0
0.5
1.0
1.5
2.0

Fig. 4

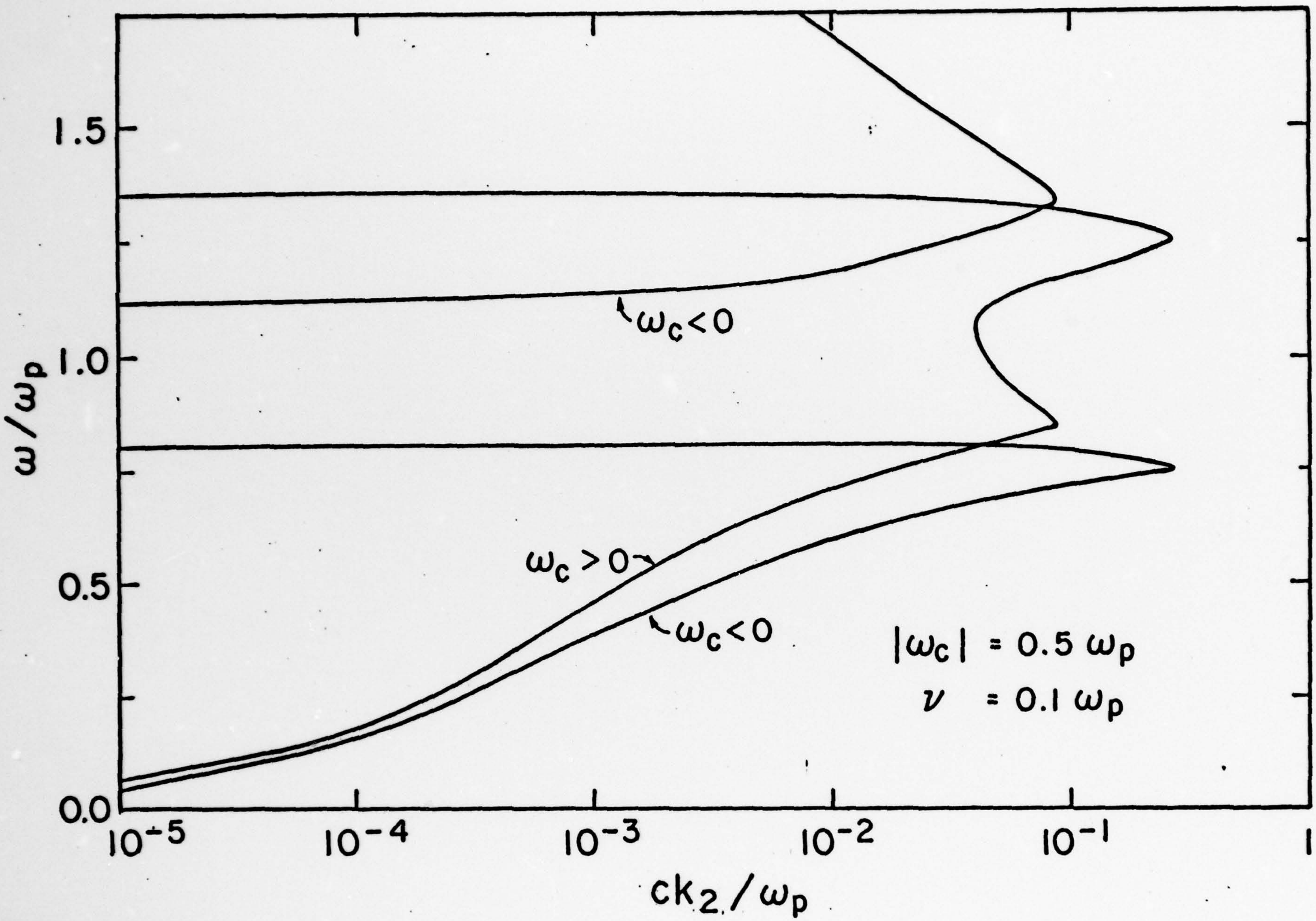

1.5
1.0
0.5
0.0
ω/ω_p
10^{-5}
10^{-4}
10^{-3}
10^{-2}
10^{-1}
1
ck_2/ω_p
$\omega_c<0$
$\omega_c>0$
$\omega_c<0$
$|\omega_c| = 0.5\,\omega_p$
$\nu = 0.1\,\omega_p$

Fig. 5

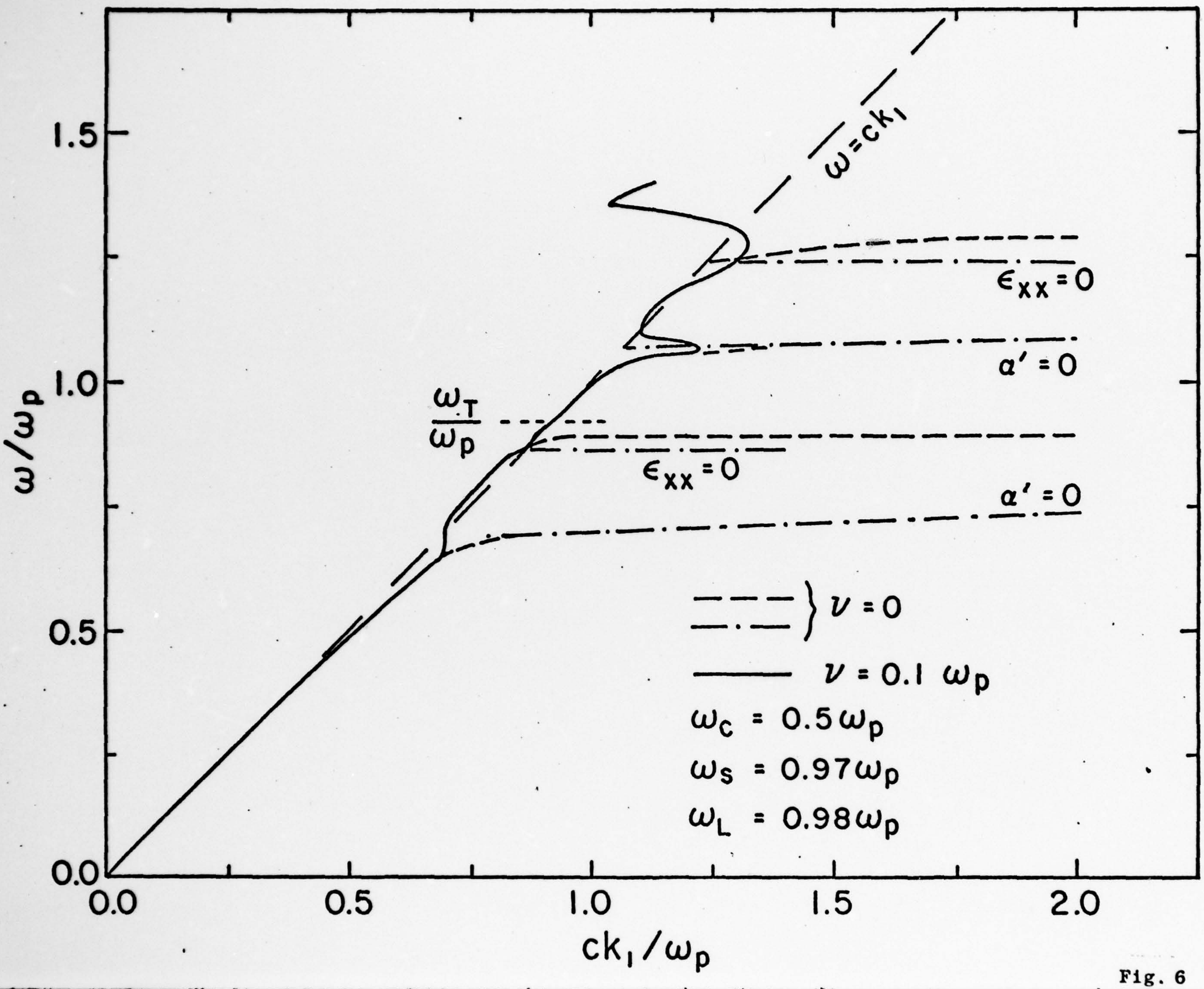

1.5
1.0
0.5
0.0
ω/ωp
0.0
0.5
1.0
1.5
2.0
ck1/ωp
ω=ck1
ϵxx=0
α′=0
ωT/ωp
ϵxx=0
α′=0
} ν=0
ν=0.1 ωp
ωc = 0.5ωp
ωs = 0.97ωp
ωL = 0.98ωp

Fig. 6

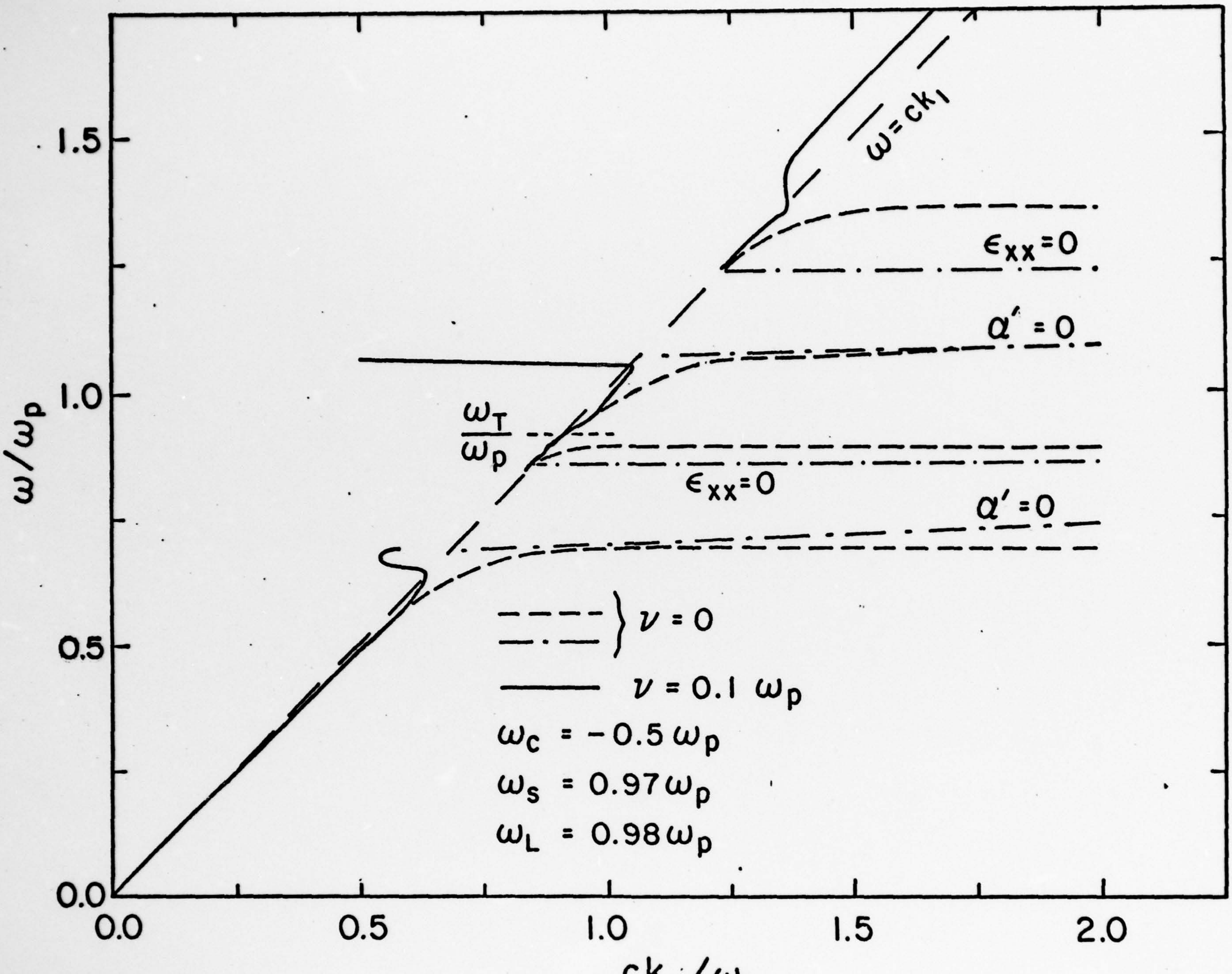

1.5
1.0
0.5
0.0
ω/ω_p
0.0
0.5
1.0
1.5
2.0
ck_1/ω_p
$\omega = ck_1$
$\epsilon_{xx}=0$
$\alpha'=0$
$\frac{\omega_T}{\omega_p}$
$\epsilon_{xx}=0$
$\alpha'=0$
$\nu = 0$
$\nu = 0.1\ \omega_p$
$\omega_c = -0.5\,\omega_p$
$\omega_s = 0.97\,\omega_p$
$\omega_L = 0.98\,\omega_p$

Fig. 7

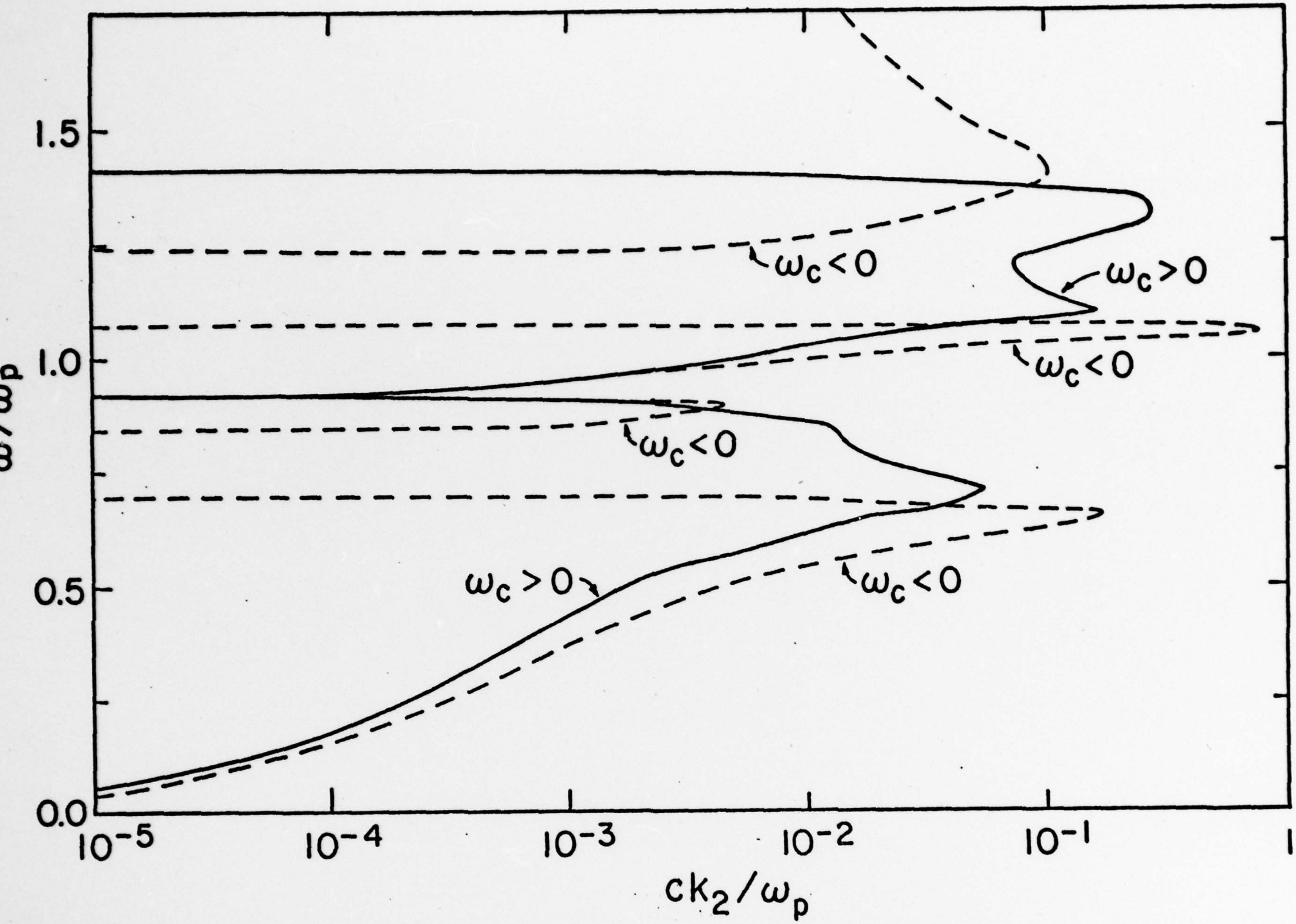

1.5
1.0
0.5
0.0
ω/ω_p
10^{-5}
10^{-4}
10^{-3}
10^{-2}
10^{-1}
1
ck_2/ω_p
$\omega_c<0$
$\omega_c>0$
$\omega_c<0$
$\omega_c<0$
$\omega_c>0$
$\omega_c<0$

Fig. 8